

Effect of NO₂ in air on the electrical conductance of In₂O₃ films with and without added ZnO prepared by R.F. Sputtering

Y. SADAOKA

Department of Industrial Chemistry, Faculty of Engineering, Ehime University, Matsuyama 790, Japan

T. A. JONES

Health and Safety Executive, Sheffield S3 7HQ, UK

W. GÖPEL

Institute of Physical and Theoretical Chemistry, University of Tübingen 7400 Tübingen, West Germany

S. KIMURA, N. HONDA

Yamatake Honeywell Co. Ltd, Fujisawa 251, Japan

The conductance of indium oxide films with and without added zinc oxide consisting of ultra-fine particles with a mean particle size of ≤ 30 nm, decreased by a factor of about 500 upon changing from air to 10 p.p.m. NO₂ in air at 150°C. The dramatic decrease in the conduction caused by NO₂ adsorption is mainly attributed to the increase in the activation energy, E , in the Arrhenius relationship $G = G_0 \exp(-E/kT)$, while the pre-exponential factor, G_0 , is almost constant. The conductance measured in air and NO₂/air for the films with and without added zinc oxide can be fitted to this relationship in the temperature range below 250°C. The decrease in the carrier concentration is considered as the origin of the decrease in conductance caused by NO₂ adsorption. The alternative explanation in terms of an increase in the grain-boundary potential, i.e. the mobility gap, can be ruled out because the depletion layer width is larger than the mean particle size.

1. Introduction

Many semiconducting materials have been used for gas sensors. It is well known that the electrical conductance of an n-type semiconductor decreases when oxidizing gases are adsorbed. Gas sensors for detecting nitrogen oxides have become of particular worldwide commercial interest. In the development of nitrogen dioxide sensors, organic compounds acting as p-type semiconductors have been studied predominantly [1-5]. However, the thermal and/or chemical stabilities of these organic compounds are generally inferior to those of metal oxides such as ZnO_x, SnO_x and In₂O_x all of which are n-type semiconductors.

It is well known that gas sensor characteristics and electrical properties of n-type semiconductors depend on the geometric structure of films or sintered bodies [6-10]. According to the grain-boundary potential model, the conductance of an n-type semiconductor decreases upon adsorption of oxidizing gases because a depletion layer is formed at the surface. As a result, an increase is achieved in the mobility barrier resulting from the band bending to higher energy. This effect is pronounced in interparticulate necks when the neck size is less and the particle size is larger than the Debye length. In films of sintered materials consisting of

ultra-fine particles with the radius of the particles below the Debye length, the depletion layer extends over the entire particles. As a result, the sensitivity to oxidative gases, i.e. the conductance changes, may not be influenced by the particle size or the film thickness. As an example, Ogawa *et al.* [8] reported the resistance of SnO_x to be inversely proportional to film thickness below 150 μ m. The resistivity decreased with decreasing oxygen pressure during film preparation by r.f. sputtering. For all samples, the mean particle size of SnO_x as determined by X-ray diffraction is less than 30 nm and decreases to 6 nm when the oxygen pressure during film preparation is decreased from 5 to 0.05 torr. In addition, the ultrafine particle films have many pores and the effective density of SnO_x in these films is about 1/600 of the value in sintered SnO_x thin films of the same thickness. In conclusion, it seems that r.f. sputtering is a suitable technique for preparing reliable gas sensing devices which are based upon ultrafine particles with a high surface area.

In the present study gas sensing characteristics of indium oxide films with and without added zinc oxide were investigated. The films were prepared by r.f. sputtering and were examined with a view to fabricating nitrogen dioxide gas sensors.

2. Experimental details

Samples were prepared using an r.f. sputtering apparatus which could be evacuated to $< 1 \times 10^{-5}$ torr. Subsequently argon–oxygen mixed gas (1 : 1) was fed into the chamber to a pressure of 0.02 torr during sputtering with 50 W. The targets were disc-shaped 99.99% pure In_2O_3 with and without 3 wt % ZnO. The sputtering rate was 4.7 nm min^{-1} for In_2O_3 and 3.4 nm min^{-1} for In_2O_3 with 3 wt % ZnO. These materials were sputtered on to alumina substrates over a pair of gold electrodes. The thickness of the sputtered film was controlled by the sputtering time. After preparation, all samples were annealed at 400°C for 64 h in air prior to the electrical and gas exposure measurements in synthetic air (< 1 p.p.m. CO, < 2 p.p.m. CO_2 , < 1 p.p.m. HCl, < 10 p.p.m. H_2O) and 10 p.p.m. NO_2 in air. The gas flow rate was maintained at 50 ml min^{-1} . The d.c. conductance was measured using a digital electrometer with d.c. power supply. The film structure was examined by X-ray diffraction (XRD) and scanning electron microscopy (SEM).

3. Results and discussion

The gas sensitivity, i.e. the variation of the conductance with gas adsorption of an n-type semiconducting sintered oxide film composed of particles with sizes larger than the Debye length is generally interpreted in terms of the change of the grain-boundary potential. The activation energy of mobility caused by the grain-boundary potential is affected by variations of the depletion layer length induced by variations of adsorbed gases. For a sample in which the size of both the neck and the particles is considerably larger than the depletion or accumulation layer width induced by gas adsorption at the surfaces, the gas sensitivity can be explained by changes in the surface conductance.

In the present work, this explanation cannot be applied since the films consist of ultrafine particles with particle sizes less than the Debye length, especially for films with zinc oxide doping.

According to the grain-boundary trapping model [11], the expected electrical properties may be divided into three different cases, I, II and III. In Fig. 1, conduction band profiles with and without trapping sites are shown.

(I) When the size (diameter) of the particle is less than the Debye length $L_d = (\epsilon kT/N_0 e^2)^{1/2}$, i.e. $L_d >$

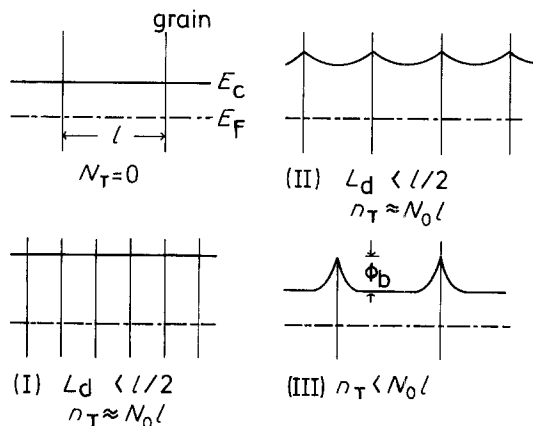


Figure 1 Conduction band profiles through a grain.

$l/2$ and $n_T \approx N_0 l$, the conduction band shifts to higher energies in the bulk and the surface of these particles so that the carrier concentration, N , and the mobility, μ , are expressed as

$$N = (N_0/N_c/N_T) \exp [-(E_c - E_T)/kT] \quad (1)$$

$$\mu = \mu_0 \quad (2)$$

Where N_0 is the density of charged doping level, N_c is the effective density of states in the conduction band, N_T is the corresponding trap density, n_T is the density per unit area of charges trapped in surface states, l is the grain size and E_T is the trap energy. In this case, the formation of the grain-boundary potential upon adsorption of oxygen or nitrogen dioxide is negligible and a decrease is expected in the carrier concentration.

(II) When $n_T \approx N_0 l$ and $L_d < l/2$, the carrier concentration and the mobility are expressed as

$$N = (2\pi)^{1/2} [L_d N_0 N_c / l (N_T - N_0)] \times \exp [-(E_c - E_T - \Phi_b)/kT] \quad (3)$$

$$\mu = \mu_0 \exp (-\Phi_b/kT) \quad (4)$$

where Φ_b is the activation energy of the mobility which corresponds to the grain-boundary potential.

(III) For $n_T < N_0 l$, the carrier concentration and the mobility are expressed as

$$N = N_0 \quad (5)$$

$$\mu = \mu_0 \exp (-\Phi_b/kT) \quad (6)$$

In this case, the carrier concentration is unaffected and the mobility gap is formed near the grain boundaries by the adsorption of oxidative gases.

In principle, the grain-boundary potential, Φ_b , decreases with decreasing depletion layer width [12]. In this case, the relation between the height of grain-boundary potential (i.e. the Schottky barrier) and the thickness of the depletion region for n-type semiconductors, which is influenced by the concentration of oxidative gases adsorbed on the particle surfaces, can be estimated as a function of the donor density, N_0 (\approx carrier concentration) when the dielectric constant, ϵ , is known. The results are shown in Fig. 2 for $\epsilon = 10$. Recently, the carrier concentration and the

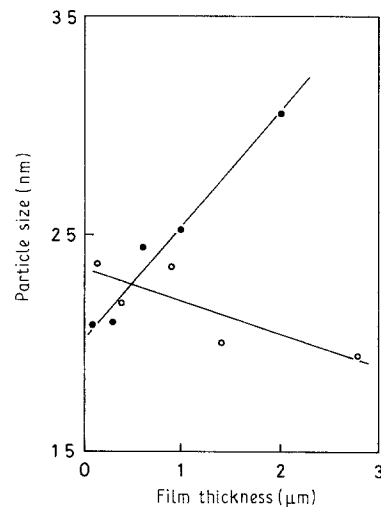


Figure 2 Correlation between particle size and film thickness for In_2O_x films (●) with and (○) without ZnO_x .

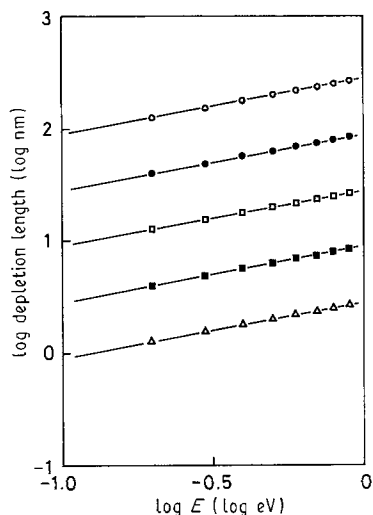


Figure 3 Relation between depletion length and grain-boundary potential height for $\epsilon = 10$. Carrier concentration: (O) 10^{16} cm^{-3} , (●) 10^{17} cm^{-3} , (□) 10^{18} cm^{-3} , (■) 10^{19} cm^{-3} , (Δ) 10^{20} cm^{-3} .

mobility for the r.f. sputtered SnO_x film have been reported by Ippommatsu and Sasaki [13]. They confirmed that the carrier concentration was strongly influenced by the adsorbed species while the mobility was almost constant in the temperature range between 300 and 500°C. In addition, the carrier concentration in air was estimated to be below 10^{17} cm^{-3} . Because the electrical properties of SnO_x resemble those of In_2O_x , it may be assumed that the carrier concentration of In_2O_x is of the same order as, and that of In_2O_x with added ZnO_x is considerably lower than that for SnO_x (probably by a factor of ~ 100). Therefore, the depletion depth may be greater than 30 nm for In_2O_x and greater than 3000 nm for In_2O_x with ZnO_x .

In Fig. 3, the correlation between the mean particle size as determined by XRD and the film thickness is shown. For In_2O_x , the mean particle size decreases monotonically with film thickness while the reverse dependence is observed for $\text{In}_2\text{O}_x\text{-ZnO}_x$. Mean particle sizes range from 30 to 20 nm. Therefore the first model ($L_d > l/2$ and $n_T \approx N_0 l$) is suitable to explain the experimental results obtained in this work.

Ideal crystalline In_2O_3 is an insulator. The high n-type conductivity observed for the polycrystalline thin films may be explained by two different mechanisms: (I) a stoichiometry deviation and (II) a doping effect of impurities. In the first case, the high n-type conductivity can be achieved without doping because

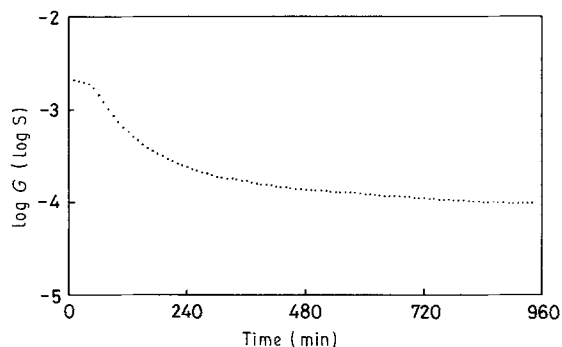


Figure 4 Change of log conductance with time in air at 250°C for annealed In_2O_x film with 3 wt % ZnO_x and 1 μm thickness.

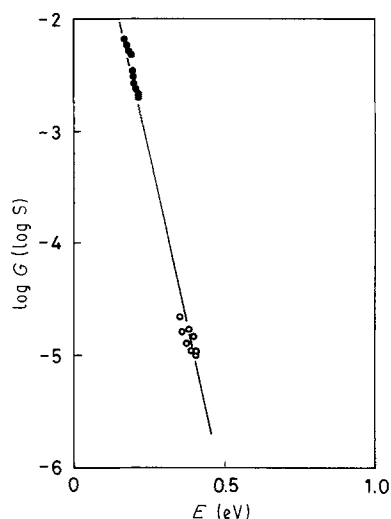


Figure 5 Correlation between log G at 150°C and activation energy for a 0.9 μm thick In_2O_x film in (●) air and (O) NO_2/air .

excess metal atoms or oxygen vacancies act as donors. The electrical conductance in indium oxide is strongly affected by the annealing conditions. Annealing in air leads to a decrease in the deviation from ideal stoichiometry because of a decrease in the concentration of oxygen vacancies. To avoid any changes in the stoichiometry deviations during the electrical measurements, all samples were therefore annealed initially in air at 400°C for 64 h and the electrical measurements were limited to the temperatures below 250°C. As a typical example, Fig. 4 shows the time dependent conductance at 250°C in air for an $\text{In}_2\text{O}_x\text{-ZnO}_x$ 1 μm thick film. It appears that the conductance in air is stabilized after about 10 h and similar behaviour was observed for the other samples. After stabilizing the conductance in air, the first cooling run down to the temperature of 120°C was started. In successive runs the temperature was changed up and down between 120 and 250°C. The conductance upon temperature increase was recorded in air and in air with 10 p.p.m. NO_2 . In this temperature region, the conductance may be expressed as

$$G = G_0 \exp(-E/kT) \quad (7)$$

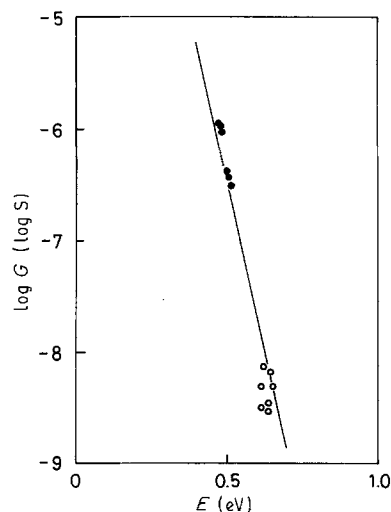


Figure 6 Correlation between log G at 150°C and activation energy for a 0.1 μm thick In_2O_x film with 3 wt % ZnO_x , in (●) air and (O) NO_2/air .

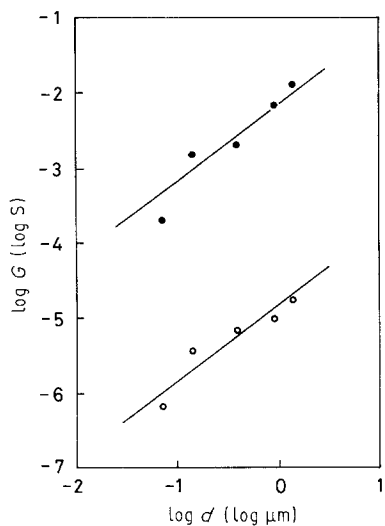


Figure 7 Thickness dependence of conductance at 150°C for In_2O_x film in (●) air and (○) NO_2/air .

For some samples only, the conductance at temperatures above 210°C deviated slightly from the value extrapolated from the lower temperature region.

In Fig. 5 the correlation between $\log G$ at 150°C and its activation energy for an In_2O_x film with $0.9\ \mu\text{m}$ thickness is shown. The slope of the solid line is $-11.9\ \text{eV}^{-1}$ which estimated from $1/kT$ at 423 K. The experimental results are well fitted to the solid line within experimental error. This good agreement indicates the pre-exponential factor in Equation 7 to be almost independent of the measuring atmosphere while the activation energy is increased when the atmosphere changes from air to NO_2/air . Similar correlations were confirmed for $\text{In}_2\text{O}_x\text{-ZnO}_x$ films. The results for a film with $0.1\ \mu\text{m}$ thickness is shown in Fig. 6. By comparing the two systems shown in Figs 5 and 6, we find the activation energy of conduction increases when zinc oxide is added to the indium oxide film. This increase in the activation energy is interpretable in terms of the lower valency cations producing holes which act as electron traps in In_2O_x . As a result, the carrier concentration is lowered by doping with ZnO_x .

Figs 7 and 8 show the thickness dependence of the

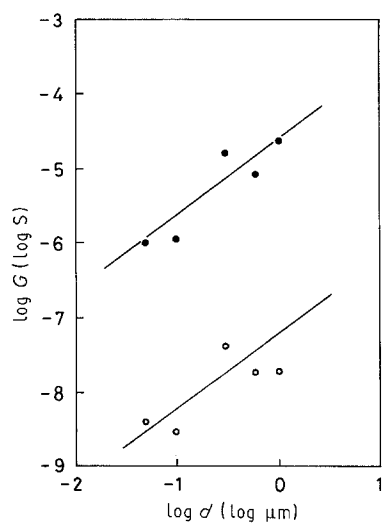


Figure 8 Thickness dependence of conductance at 150°C for In_2O_x film with 3 wt % ZnO_x in (●) air and (○) NO_2/air .

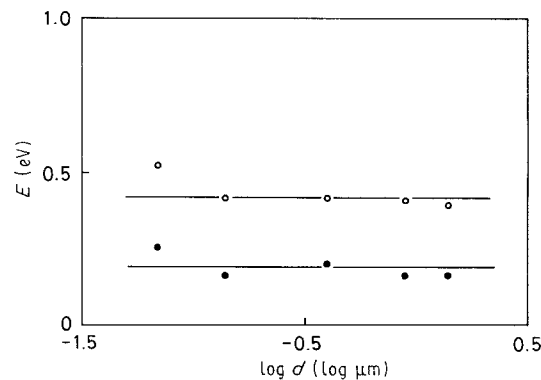


Figure 9 Thickness dependence of activation energy for In_2O_x film in (●) air and (○) NO_2/air .

conductance at 150°C. The observed conductance under each condition is proportional to the film thickness. The ratio of conductance in air and in NO_2/air is almost independent of the thickness. It is estimated to be 600 for indium oxide films and 330 for indium oxide films containing 3 wt % zinc oxide. The correlation between the activation energy of conduction observed in the temperature range from 120 to 200°C and the film thickness is shown in Figs 9 and 10. For indium oxide films, the activation energy observed under the same conditions is almost independent of the film thickness, while the value for the $0.07\ \mu\text{m}$ thick In_2O_x film is slightly higher. The difference, however, between the activation energies is independent of the film thickness and is estimated to be $0.24 \pm 0.02\ \text{eV}$. By assuming that the pre-exponential factor in Equation 7 is proportional to the film thickness and independent of the ambient atmosphere, the value of the ratio of conductance in air and that in NO_2/air mixture at 150°C is estimated to be 700. This is in good agreement with the observed value of 600 for which the corresponding difference in activation energies is $0.233\ \text{eV}$. For indium oxide containing 3 wt % zinc oxide, the activation energy in air is only slightly affected by the film thickness and is estimated to be $0.44 \pm 0.04\ \text{eV}$ while a gradual increase in the activation energy with the film thickness is observed in the NO_2/air mixture. The mean activation energy for an NO_2/air mixture is shown in Fig. 10 by the broken line. In this figure, the interpolated values are estimated

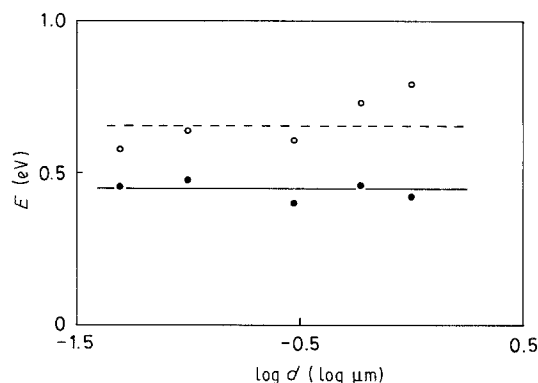


Figure 10 Thickness dependence of activation energy for In_2O_x film with 3 wt % ZnO_x in (●) air and (○) NO_2/air . (---). Estimated value from the conductances in air and NO_2/air and the activation energy in conductance in air.

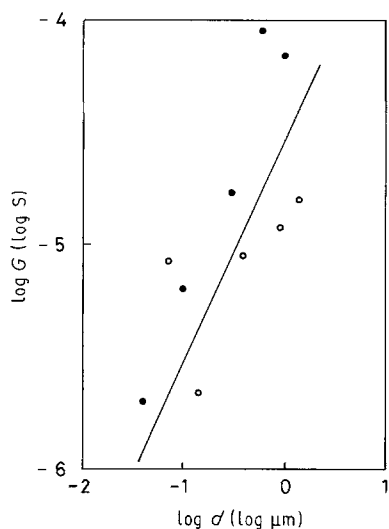


Figure 11 Thickness dependence of conductance at 150°C for $E = 0.4\text{ eV}$ for In_2O_3 film (●) with and (○) without ZnO_x .

from the conductances in air and NO_2/air at 150°C and the activation energy in air (0.44 eV) by using Equation 7 in which the pre-exponential factor is proportional to the film thickness and assumed to be unaffected by the atmosphere. This interpretation of activation energy data indicates that the conductance decrease in the presence of NO_2 is primarily caused by an increase in the activation energy.

The thickness dependence of interpolated value of $\log G$ for $E = 0.4\text{ eV}$ at 150°C is shown in Fig. 11. $\log G$ is linearly proportional to the logarithm of film thickness and almost unaffected by the doping with zinc oxide. This result indicates that the introduction of a lower valency cation produces a hole which acts as an electron trap while the pre-exponential factor is hardly influenced. Furthermore, the mechanism by which the activation energy is increased when zinc oxide added to the bulk is similar to that which occurs when oxidative gases are adsorbed on the surface of ultrafine particles. This similarity results from the fact that the Debye length in oxidative gases is greater than the particle size.

4. Conclusions

R.f. sputtered indium oxide films are suitable for the detection of NO_2 in air. The change in the conductance with the adsorption of NO_2 is caused by an increase in the activation energy of conduction while the pre-exponential factor is almost unaffected. The conductance at 150°C decreases by a factor of about 500 upon changing from air to 10 p.p.m. NO_2 in air. Under identified atmospheric conditions the conductance is proportional to the film thickness. The doping of a lower valency cation such as zinc leads to an increase in the activation energy of conduction. The difference, however, in the activation energies of conduction in air and in NO_2/air is not affected.

References

1. R. L. VAN EWYK, A. V. CHADWICK and J. D. WRIGHT, *J. C. S. Faraday I* **76** (1980) 2194.
2. C. L. HONEYBOURNE and R. J. EWIN, *J. Phys. Chem. Solids*, **44** (1983) 215.
3. B. BOTT and T. A. JONES, *Sensors and Actuators* **5** (1984) 43.
4. T. A. JONES and B. BOTT, *ibid.* **9** (1986) 27.
5. Y. SADAOKA, Y. SAKAI, N. YAMAZOE and T. SEIYAMA, *Denki Kagaku* **50** (1982) 457.
6. T. SUZUKI, T. YAMAZAKI, H. YOSHIOKA and K. HIKICHI, *J. Mater. Sci.* **23** (1988) 145.
7. J. L. VOSSEN and E. S. POLNIAK, *Thin Solid Films* **13** (1972) 281.
8. H. OGAWA, A. ABE, M. NISHIOKA and S. HAYAKAWA, *J. Electrochem. Soc.* **128** (1981) 2020.
9. H. PINK, L. TREITINGER and L. VITÉ, *Jpn. J. Appl. Phys.* **19** (1980) 513.
10. S. RI, K. HAMANO and Z. NAKAGAWA, *Yogyo Kyokaishi* **94** (1986) 43.
11. K. L. CHOPRA, S. MAJOR and D. K. PANDYA, *Thin Solid Films* **102** (1983) 1.
12. C. A. MILLER, *J. Phys. D. Appl. Phys.* **4** (1971) 690.
13. M. IPPOMMATSU and H. SASAKI, *Denki Kagaku* **56** (1988) 451.

Received 16 February
and accepted 24 August 1989